UDK 620.1:67.017:669.35
Original scientific article/Izvirni znanstveni članek

ISSN 1580-2949
MTAEC9, 55(4)483(2021)

PHASE-TRANSFORMATION DYNAMICS AND CHARACTERIZATION OF PRECIPITATES IN THE Cu-3Ti-3Ni-0.5Si ALLOY

DINAMIKA FAZNE TRANSFORMACIJE IN KARAKTERIZACIJA IZLOČKOV ZLITINE Cu-3Ti-3Ni-0,5Si

Jia Liu[1*], Jituo Liu[2], Xianhui Wang[2], Chong Fu[1], Yanlong Wang[1], Linlin Lu[1], Jing Zheng[3]

[1]School of Materials Science and Engineering, Xi'an Polytechnic University, No.19 South Jinhua Rd., Xi'an 710048, China
[2]School of Materials Science and Engineering, Xi'an University of Technology, No.5 South Jinhua Rd., Xi'an 710048, China
[3]Shaanxi Institute for Materials Engineering, Northwest Institute for Non-ferrous Metal Research, No.96 Wei Yang Rd., Xi'an 710016, China

Prejem rokopisa – received: 2020-08-22; sprejem za objavo – accepted for publication: 2021-03-26

doi:10.17222/mit.2020.166

In this paper we investigated the phase-transformation dynamics of the Cu-3Ti-3Ni-0.5Si alloy by applying the Avrami method to phase-transformation dynamics and electrical conductivity based on the relationship between the electrical conductivity and the volume fraction of precipitates in the Cu-3Ti-3Ni-0.5Si alloy. The results corroborated well with the experimental data. The microstructure and precipitated phases were characterized by scanning electron microscopy (SEM) and transmission electron microscopy (TEM). The analysis of the selected-area electron-diffraction patterns indicated that the precipitates formed in the matrix of the Cu-3Ti-3Ni-0.5Si alloy during aging, correspond to the Ni_3Ti, Ni_3Si, and Ni_2Si phases. According to the values of formation enthalpy and cohesive energy determined by first-principle calculations, the formation of the Ni_2Si phase is more favorable compared to the Ni_3Si and Ni_3Ti phases, and the Ni_3Ti exhibits improved structural stability compared to the Ni_2Si and Ni_3Si phases.

Keywords: copper alloy, phase-transformation dynamics, precipitates, structural stability

Avtorji v članku opisujejo raziskavo dinamike faznih transformacij (pretvorb) zlitine Cu-3Ti-3Ni-0,5Si z uporabo Avramijeve metode dinamike faznih transformacij na osnovi zveze med električno prevodnostjo in volumskim deležem izločkov v zlitini Cu-3Ti-3Ni-0,5Si. Dobljeni rezultati se dobro ujemajo z eksperimentalnimi podatki. Avtorji so mikrostrukturo in izločene faze okarakterizirali z vrstičnim in presevnim elektronskim mikroskopom (SEM in TEM). Analize dobljenih elektronskih vzorcev sipanja rentgenskih žarkov na posameznih izbranih področjih kažejo, da so izločki nastali v kovinski osnovi med staranjem zlitine Cu-3Ti-3Ni-0.5Si tipa Ni_3Ti, Ni_3Si in Ni_2Si. Glede na izračunane vrednosti za tvorbeno entalpijo in kohezivno energijo ima tvorba Ni_2Si faze prednost pred fazama Ni_3Si in Ni_3Ti. Faza Ni_3Ti ima boljšo strukturno stabilnost v primerjavi s fazama Ni_2Si in Ni_3Si.

Ključne besede: zlitina na osnovi bakra, dinamika fazne transformacije, izločki, strukturna stabilnost

1 INTRODUCTION

Copper alloys with high strength and electrical conductivity are indispensable new structural and functional materials in high-tech fields, such as microelectronics, aviation, aerospace, and communications.[1–3]

Although previous studies reported the successful synthesis of Cu-Ni-Si alloys, Cu-Ni-Sn alloys, Cu-Mg-Ca alloys, and Cu-Ag alloys, the realization of high strength and high electrical conductivity in a single copper alloy remained unresolved.[4–7] The strengthening of traditional copper alloys, such as Cu-Be, relies on aging precipitation to achieve high strength and electrical conductivity. The aging precipitation process purifies the alloy, which improves the electrical conductivity, but the method fails to simultaneously improve the electrical conductivity and strength.[8] The strength of copper alloys depends on the immobility of dislocations, which requires a high density of the precipitated nano-phase in the alloy. This limits the purification of the copper alloy matrix, and thus reduces the final electrical conductivity.

The Cu-Ti alloy has high strength and hardness, good resistance to corrosion and to wear, and a low production cost. However, dissolved Ti atoms in the Cu matrix enhances the electron scattering, which substantially reduces the electrical conductivity of the Cu-Ti alloy and limits its application. Thus, the improvement of electrical conductivity without deteriorating the excellent mechanical response of Cu-Ti alloys is of utmost importance for the successful development of functional Cu-Ti alloys.[9,10] The electrical conductivity of Cu-Ti alloys can be increased by reducing the electron scattering, which can be achieved via the reduction of the amount of Ti solute atoms and alloying elements in the alloy. Based on this research idea, alloying elements such as Cr, Sn, Si and P were added to a Cu-Ti alloy. However, without substantial improvements in the electrical conductivity.[11–14]

*Corresponding author's e-mail:
785576187@qq.com (Jia Liu)

The addition of Ni and Si to Cu-Ti alloys enhanced the electrical conductivity, but still, the adverse relation between high strength and high electrical conductivity was not avoided.[15] The investigation of the dynamics of phase transformation and precipitation characteristics of the Cu-3Ti-3Ni-0.5Si alloy is of great significance for the selection of the appropriate heat treatment to achieve optimal functional properties. In the present work, the phase-transformation dynamics of the Cu-3Ti-3Ni-0.5Si alloy was studied using the Avrami method for phase-transformation kinetics and electrical conductivity. In addition, the microstructure and precipitated phases were characterized by scanning electron microscopy and transmission electron microscopy. The present work aims to synthesize a new Cu alloy with an optimal relation between mechanical strength and electrical conductivity.

2 EXPERIMENTAL PART

We used a vacuum induction furnace (ZG-25) to fabricate an ingot of Cu-3 *w*/%, Ti-3 *w*/%, Ni-0.5 *w*/%, Si alloy with a diameter of 110 mm. After the ingot scalping, it was homogenized at 800 °C for 120 min and solubilized at 850 °C for 240 min in an electrical resistance furnace (SK-G10123K), followed by quenching into water. Then, the specimens were aged at (400, 450, 500, 550) °C for (15, 30, 45, 60, 90, 120, 150, 180, 240, 300, 360, 480, 600, 840, 1080) min. An eddy conductivity gauge (FQR-7501) was used to determine the electrical conductivity, and the morphology and precipitated phases were characterized using a scanning electron microscope (Zeiss-Merlin) and a transmission electron microscope (JEM-3010) operating at 200 kV. We used a precision saw (Somet1000) to cut the specimens for the TEM analysis, and then mechanically polished them down to 50-μm-thick slices. From these slices, we punched 3-mm-discs and ion-milled them at 4.5 kV (Fischione1010).

3 RESULTS AND DISCUSSION

3.1 Dynamics of phase transformation

During the aging treatment, the electrical conductivity (the unit of electrical conductivity is %IACS.) steadily rises with an increase of the aging time. Before the aging treatment, the electrical conductivity is denoted σ_0 and the volume fraction of the precipitated phase is $f = 0$.

After a reasonably long aging time, the precipitation is completed, and the electrical conductivity reaches σ_{max} and the volume fraction of the precipitated phase is $f = 1$. The relationship between the electrical conductivity (σ) and the volume fraction of the precipitated phase (f) is linear, which can be expressed as:

$$\sigma = \sigma_0 + Af \tag{1}$$

$$A = \sigma_{max} - \sigma_0 \tag{2}$$

The value of σ can be measured during the aging for different times, and the volume fraction of the precipitated phase can be calculated using Equations (1)–(2).

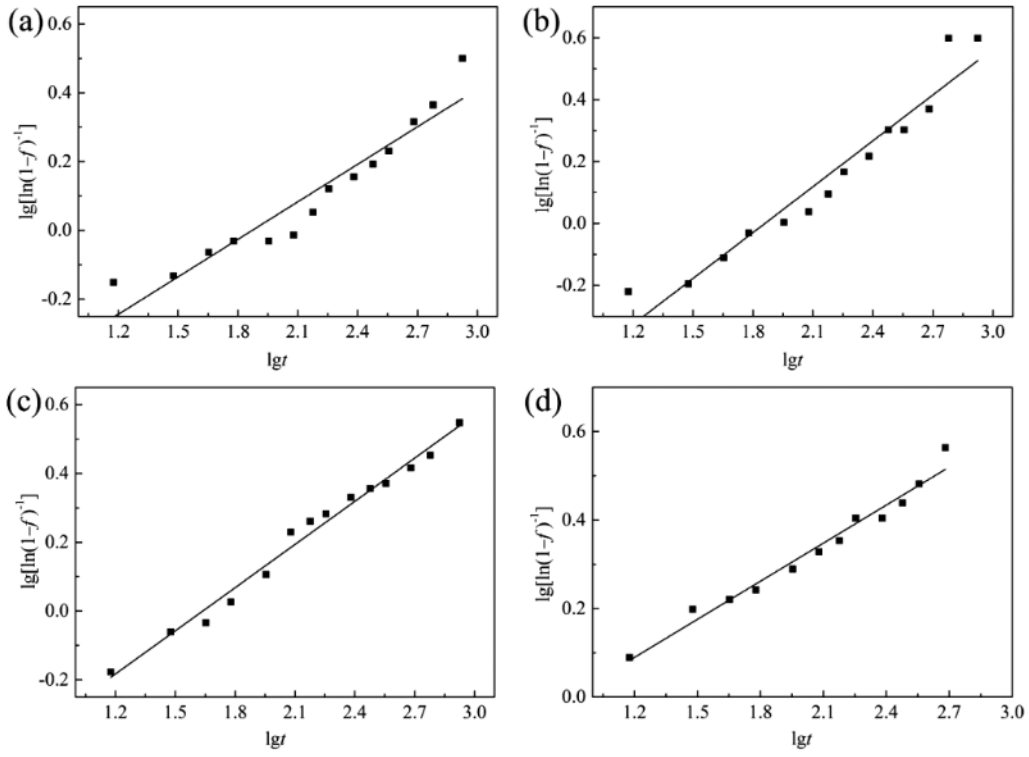

Figure 1: Curve of lg [ln $(1 - f)^{-1}$] and lg$t$ in isothermal aging course: a) 400 °C; b) 450 °C; c) 500°C; d) 550 °C

The relationship between the volume fraction of the precipitated phase, f, and the aging time, t, can be expressed as follows:

$$f = 1 - \exp(-bt^n) \quad (3)$$

where b and n are constants. The parameter b depends on the composition of the supersaturated solid solution and the temperature of the phase transformation, while n depends on the nucleation location and the type of phase transformation.[16]

Using Equations (1)–(3), we can express the electrical conductivity from Equation (1) as follows:

$$\sigma = \sigma_0 + (\sigma_{max} - \sigma_0)[1 - \exp(-bt^n)] \quad (4)$$

Furthermore, Equation (3) can be expressed as follows:

$$1 - f = \exp(-bt^n) \quad (5)$$

After being transposed, Equation (5) becomes:

$$\lg [\ln(1 - f)^{-1}] = \lg b + n \lg t \quad (6)$$

The relationship between $\lg [\ln(1 - f)^{-1}]$ and $\lg t$, **Figure 1**, is approximately a straight line, which we can use to determine the $\lg b$ as the intercept and n as the slope of the line.

The Avrami method applied to the electrical conductivity for the Cu-3Ti-3Ni-0.5Si alloy aged at (400, 450, 500, 550) °C is expressed as follows:

$$\sigma = 9.3 + 12.25\ [1 - \exp(-0.2086\ t^{0.3637})] \quad (7)$$

$$\sigma = 9.3 + 17.94\ [1 - \exp(-0.1205\ t^{0.4942})] \quad (8)$$

$$\sigma = 9.3 + 23.46\ [1 - \exp(-0.2067\ t^{0.4182})] \quad (9)$$

$$\sigma = 9.3 + 21.73\ [1 - \exp(-0.5560\ t^{0.2870})] \quad (10)$$

The Avrami method applied to the phase transformation kinetics for the Cu-3Ti-3Ni-0.5Si alloy aged at (400, 450, 500, 550) °C is expressed as follows:

$$f = 1 - \exp(-0.2086\ t^{0.3637}) \quad (11)$$

$$f = 1 - \exp(-0.1205\ t^{0.4942}) \quad (12)$$

$$f = 1 - \exp(-0.2067\ t^{0.4182}) \quad (13)$$

$$f = 1 - \exp(-0.5560\ t^{0.2870}) \quad (14)$$

This enables a calculation of the electrical conductivity for the corresponding aging time. **Figure 2** shows good agreement between the experimental results and the predicted values of electrical conductivity.

Figure 3 shows the curves of the Cu-3Ti-3Ni-0.5Si alloy based on the Avrami method applied to the kinetics phase transformation. The volume fraction of the precipitate increases with the temperature. To reach a volume fraction of precipitate in the alloy of 80 % after aging at (400, 450, 500, 550) °C, time intervals of (300, 180, 150, 45) min were required, respectively.

Both the electrical conductivity and the volume fraction of precipitate increase when the solute atoms precipitate from the supersaturated solid solution during the aging treatment. However, the density of the solute atoms decreases, so the electrical conductivity and transformation rate become constant for long aging times.

Kenta reported that the precipitated phase continued to grow in granular, strip-like, and flake morphology, or

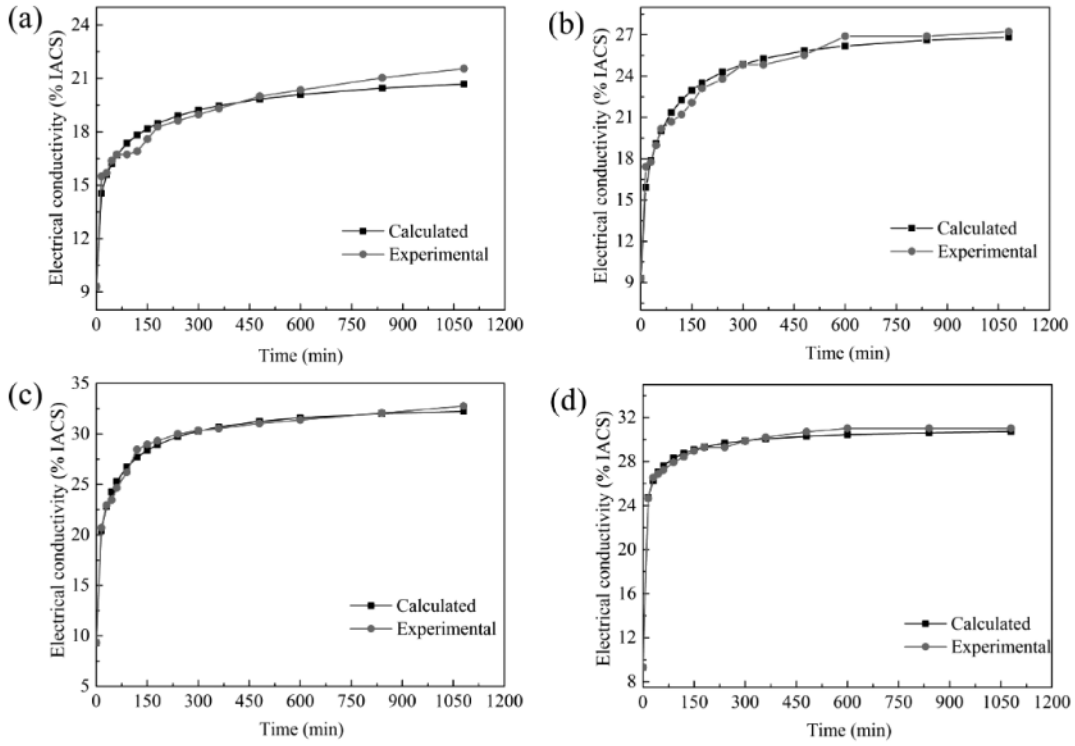

Figure 2: Predicted and experimental electrical conductivity of Cu-3Ti-3Ni-0.5Si with different temperatures: a) 400 °C, b) 450 °C, c) 500 °C, d) 550 °C

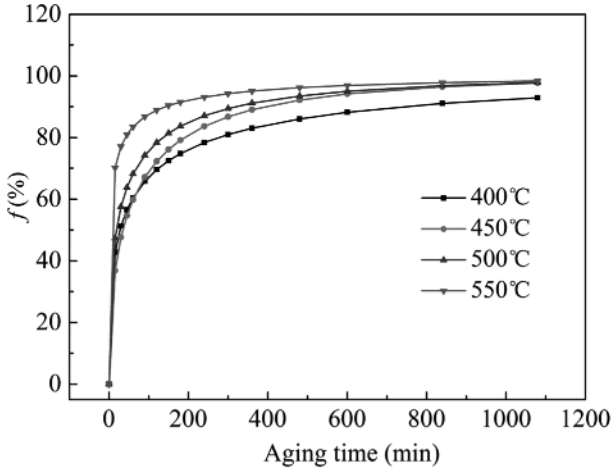

Figure 3: Influence of aging time on the volume fraction of precipitates with different temperatures

cylindrical morphology, when n (1~1.5), n = 0.5, n = 1, respectively.[17] The n value in the equation of the aging treatment of Cu-3Ti-3Ni-0.5Si alloy at different temperatures is close to 0.5. The precipitated phases for the contacts between each other via their edges, which prevents the further forward extensions of the edges. Therefore, a plausible growth mechanism for the precipitated phase is thickening of the stripe phase. The phase morphology and constituents of the precipitated phases are characterized in the next section.

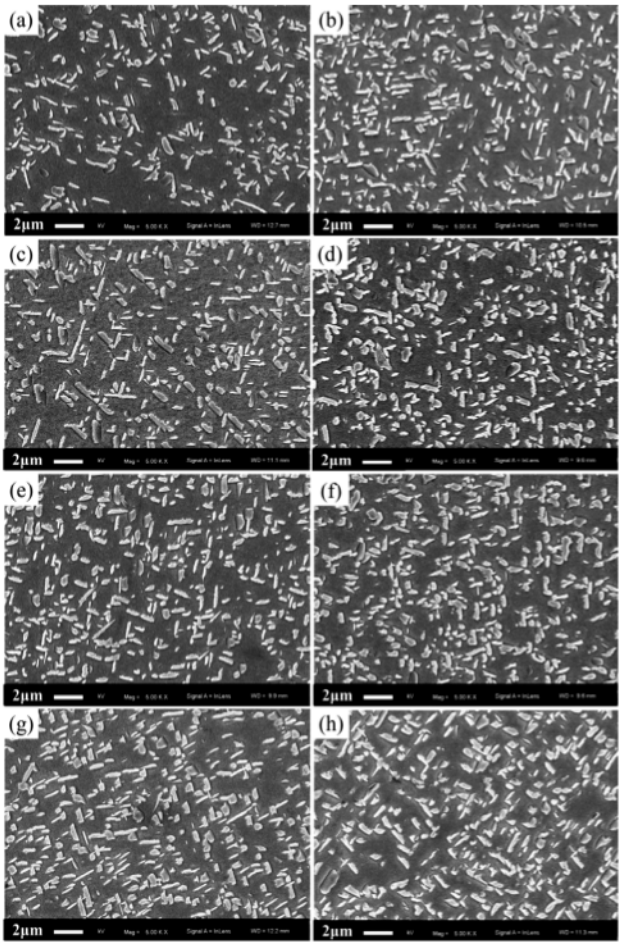

Figure 4: SEM micrograph of Cu-3Ti-3Ni-0.5Si alloy after aging at 500 °C with different time: a) 60 min, b) 120 min, c) 180 min, d) 240 min, e) 300 min, f) 360 min, g) 480 min, h) 600 min

3.2 Microstructural characterization

Figure 4 presents SEM micrographs of the Cu-3Ti-3Ni-0.5Si alloy after aging at 500 °C for different times. The majority of the precipitated phase has a stripe-like morphology. With an increase of the aging time, the striped precipitates enlarge and coarsen.

To understand the phase morphology and constituents in detail, we investigated the microstructure for the Cu-3Ti-3Ni-0.5Si alloy after aging at 500 °C for 120 min and 300 min using the TEM method. The results are shown in **Figures 5** to **7**.

TEM micrographs, **Figure 5a**, **Figure 5c**, and the corresponding SAED patterns, **Figure 5b**, **Figure 5d**, of the Cu-3Ti-3Ni-0.5Si alloy after aging at 500 °C for 120 min show that the precipitates mostly have a strip-like morphology, with a strip width of approximately 150 nm. The striped precipitates are perpendicular to each other. This morphology corresponds to the Ni_3Ti phase, **Figure 5b**, with a hexagonal crystal structure with lattice parameters of a = 0.5092 nm, b = 0.5092 nm and c = 0.8297 nm. **Figure 5c** shows that the particles in the Cu matrix originate from Ni_3Si, **Figure 5d**, which has a monoclinic crystal structure with lattice parameters of a = 0.697 nm, b = 0.625 nm, and c = 0.507 nm.

For the aging time of 300 min, the precipitates can be seen in the bright-field micrographs, as shown in **Fig-**

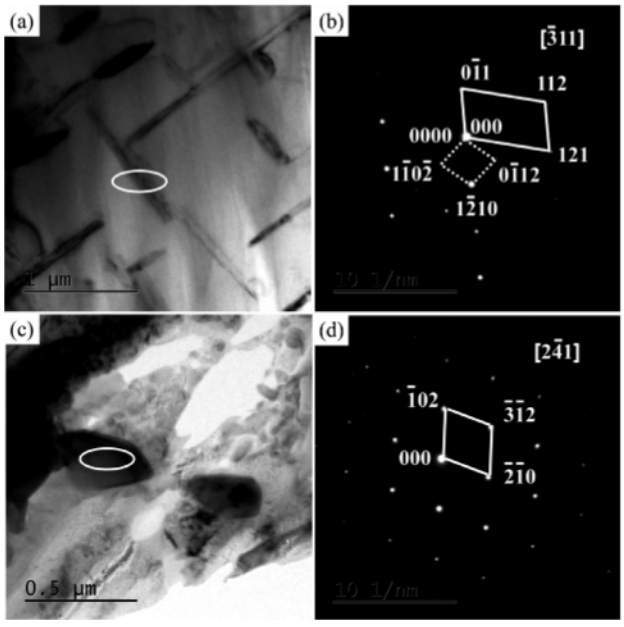

Figure 5: TEM images (a, c) and corresponding SAED patters (b, d) of Cu-3Ti-3Ni-0.5Si alloy aging at 500 °C for 120 min

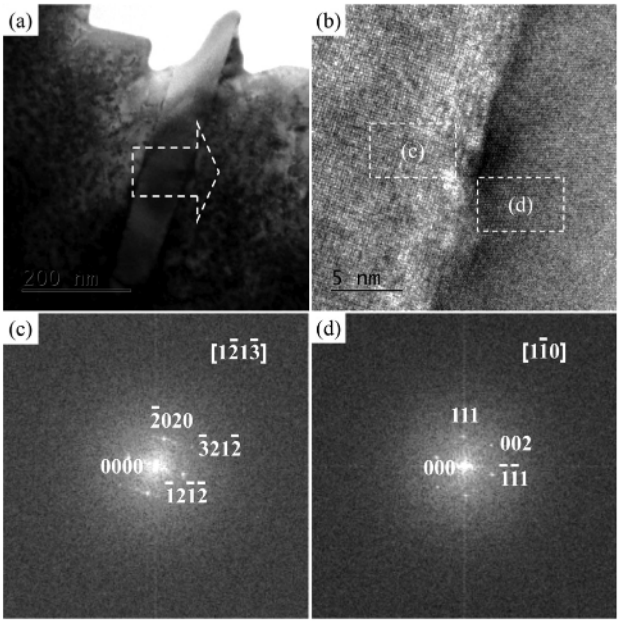

Figure 6: TEM image (a), HRTEM of precipitate phase and Cu matrix (b) and corresponding fourier transform graph of HRTEM image (c, d) of Cu-3Ti-3Ni-0.5Si alloy aging at 500 °C for 300 min

ure 6a, **Figure 7a**, and **Figure 7c**. **Figure 6a** and **Figure 6b** show TEM and HRTEM micrographs of the precipitated phase and the Cu matrix, and the corresponding Fourier transformation of the HRTEM image, **Figure 6c** and **Figure 6d**. It can be seen that the interface between the precipitate with the strip-like morphology, Ni_3Ti, and the Cu matrix is well developed. TEM images, **Figure 7a** and **Figure 7c**, and the corresponding SAED patterns, **Figure 7b** and **Figure 7d**, indicate that the particles correspond to Ni_3Si, while the spherical precipitates are Ni_2Si. It has an orthogonal crystal structure with lattice parameters of $a = 0.499$ nm, $b = 0.372$ nm and $c = 0.703$ nm. Conclusively, for the investigation of phase transformations, we can say that the stripe-like Ni_3Ti phase and the particle-like Ni_3Si phase precipitate in the alloy matrix during the initial aging stages, while longer aging times favor the precipitation of the spherical Ni_2Si phase in the matrix.

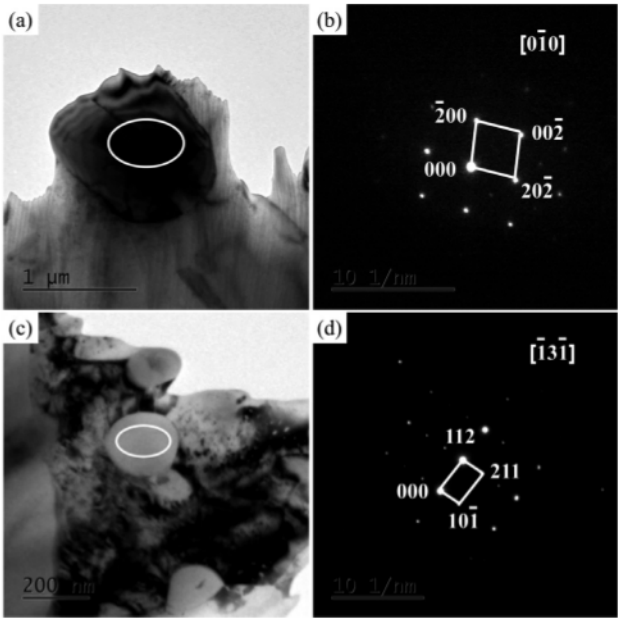

Figure 7: (a, c) TEM images and (b, d) corresponding SAED patters of Cu-3Ti-3Ni-0.5Si alloy aging at 500 °C for 300 min

3.3 Formation sequence and structural stability of the precipitates

The calculations were performed using electronic density functional theory (DFT) within the Vienna ab-initio simulation package (VASP), using the Projector Augmented Wave (PAW) potentials and the Generalized Gradient Approximation (GGA) of Perdewe Burkee Ernzerhof (PBE) scheme as supplied.[18] The plane-wave cut-off energy of 520 eV was used for Ni_3Ti, Ni_3Si, and Ni_2Si. For Brillouin-zone sampling, we adopted a $5 \times 5 \times 3$ Monkhorst-Pack mesh for Ni_3Ti, a $5 \times 4 \times 6$ Monkhorst-Pack mesh for Ni_3Si, and a $6 \times 5 \times 3$ Monkhorst-Pack mesh for Ni_2Si.[19–21] Finest grids and a higher energy cut-off (520 eV) were adopted, with the precision of energy convergence of 10^{-4} eV. The position of atoms was relaxed until the maximum force on each atom was less than 10^{-3} eV/Å.

The results of the theoretical calculations revealed that after the aging treatment, the Ni_3Ti, Ni_2Si, and Ni_3Si precipitate from the Cu matrix as major phases. To understand the precipitation mechanism, we investigated the formation sequence and structural stability of the precipitates. The cohesive energy values (ΔE) and enthalpy of formation values (ΔH) of the precipitates were calculated based on first-principles calculations. For example, for an arbitrary intermetallic A_xB_y (x and y are the total number of A and B atoms in the cell, respectively), the ΔE and ΔH can be calculated using the following expression:

$$\Delta E(A_xB_y) = [E_{AB(tot)} - xE_{A\ (atom)} - yE_{B(atom)}]/(x+y) \quad (15)$$

$$\Delta H(A_xB_y) = [E_{AB(tot)} - xE_{A\ (solid)} - yE_{B(solid)}]/(x+y) \quad (16)$$

where $E_{AB(tot)}$ is the total energy of the precipitates for an equilibrium lattice constant, $E_{A(atom)}$ and $E_{B(atom)}$ are the isolated atomic energies, and $E_{A(solid)}$ and $E_{B(solid)}$ are the solid atomic energy of the pure constituents.[22,23] The calculation indicates that the cohesive energy of the Ni_3Ti phase (–5.2011 eV/atom) is less than that of the Ni_2Si (–5.0548 eV/atom) and Ni_3Si (–4.8774 eV/atom) phases, demonstrating that the Ni_3Ti phase has better structural stability than Ni_2Si and Ni_3Si phases. However, the formation enthalpy of the Ni_2Si phase (–0.6175 eV/atom) is less than that of Ni_3Si (–0.4607 eV/atom) and Ni_3Ti (–0.5419 eV/atom), implying that the Ni_2Si phase is more likely to form than Ni_3Si and Ni_3Ti. Comparing the calculated values of the formation enthalpies, our results are in very good agreement with the previous theoretical

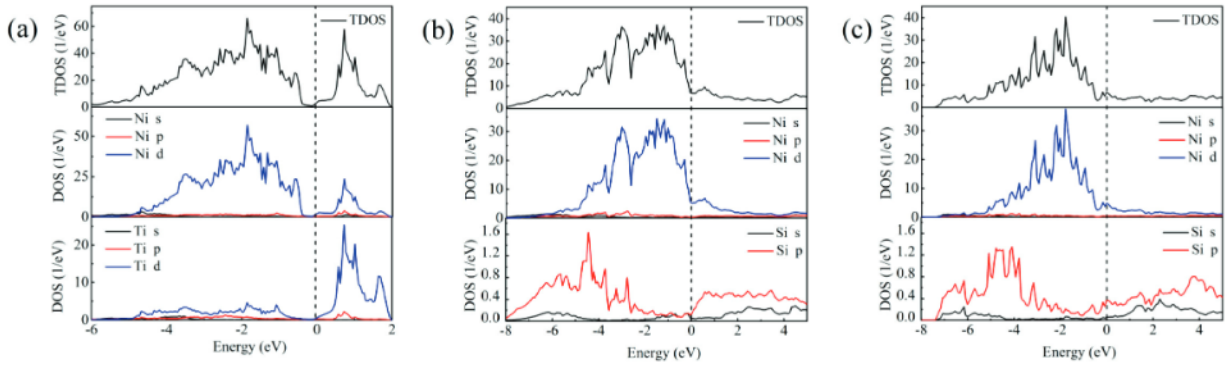

Figure 8: Density of states: a) Ni_3Ti, b) Ni_3Si, c) Ni_2Si

results, confirming the reliability of our calculation methodology.[24,25]

To further clarify the bonding characteristics and structural stabilities of the Ni_3Ti, Ni_3Si, and Ni_2Si phases, we calculated the total density of state (TDOS) and partial density of state (PDOS), as shown in **Figure 8**. The n (E_f) is positively correlated with the stability of the phase.[26] The TDOS values of the Ni_3Ti, Ni_3Si, and Ni_2Si phases are different at the Fermi level, being of (3.28, 6.717, and 6.57) states/eV, respectively. This indicates better stability of the Ni_3Ti phase than of the Ni_3Si and Ni_2Si phases.

4 CONCLUSIONS

Based on experiences and analyses of the obtained results, the following conclusions could be drawn:

- The Avrami method was applied to the phase-transformation dynamics and electrical conductivity of the Cu-3Ti-3Ni-0.5Si alloy, and the results corroborate well with the experimental data.
- The volume fraction of precipitates in the Cu-3Ti-3Ni-0.5Si alloy increases with the aging time, and these precipitates correspond to Ni_3Ti, Ni_3Si, and Ni_2Si phases according to the analysis of selected-area diffraction patterns.
- The calculated values of the formation enthalpy and cohesive energy indicate that the formation of the Ni_2Si phase is more favorable than that of the Ni_3Si and Ni_3Ti phases, but the structural stability of the Ni_3Ti phase is better than that of the other two phases.

Acknowledgment

This research was supported by the National Natural Science Foundation of China (No. 51971173), the Natural Science Basis Research Plan in Shaanxi Province of China (No.2020JQ-827) and the Education Department Foundation of Shaanxi, China (No.18JK0348).

5 REFERENCES

[1] A. Guwer, R. Nowosielski, A. Lebuda, Properties and structure of Cu-Ti-Zr-Ni amorphous powders prepared by mechanical alloying, Mater. Tehnol., 49 (**2015**) 3, 423–427, doi:10.17222/mit.2014.119

[2] R. Nowosielski, A. Guwer, K. Matus, Influence of Mechanical-alloying Parameters on the Structure and Properties of $Cu_{47}Ti_{34}Zr_{11}Ni_8$, Mater. Tehnol., 54 (**2020**) 4, 425–431, doi:10.17222/mit.2015.345

[3] Y. X. Liu, L. Wang, K. Jiang, S. T. Yang, Electro-deposition preparation of self-standing Cu-Sn alloy anode electrode for lithium ion battery, Journal of Alloys and Compounds, 775 (**2019**), 818–825, doi:10.1016/j.jallcom.2018.10.207

[4] S. Suzuki, N. Shibutani, K. Mimura, M. Isshiki, Y. Waseda, Improvement in strength and electrical conductivity of Cu-Ni-Si alloys by aging and cold rolling, Journal of Alloys and Compounds, 417 (**2006**), 116–120, doi:10.1016/j.jallcom.2005.09.037

[5] B. M. Luo, D. X. Li, C. Zhao, Z. Wang, Z. Q. Luo, W. W. Zhang, A low Sn content Cu-Ni-Sn alloy with high strength and good ductility, Materials Science and Engineering A, 746 (**2019**), 154–161, doi:10.1016/j.msea.2018.12.120

[6] M. Z. Ma, Z. Li, W. T. Qiu, Z. Xiao, Z. Q. Zhao, Y. B. Jiang, Microstructure and properties of Cu-Mg-Ca alloy processed by equal channel angular pressing, Journal of Alloys and Compounds, 788 (**2019**), 50–60, doi:10.1016/j.jallcom.2019.01.335

[7] R. Li, X. W. Zuo, E. G. Wang, Influence of thermomechanical process and Fe addition on microstructural evolution and properties of Cu-26 wt% Ag composite, Journal of Alloys and Compounds, 773 (**2019**), 121–130, doi:10.1016/j.jallcom.2018.09.179

[8] Y. J. Zhou, K. X. Song, J. D. Xing, Y. M. Zhang, Precipitation behavior and properties of aged Cu-0.23Be-0.84Co alloy, Journal of Alloys and Compounds, 658 (**2016**), 920–930, doi:10.1016/j.jallcom.2015.10.290

[9] S. Suzuki, K. Hirabayashi, H. Shibata, K. Mimural, M. Isshiki, Y. Waseda, Electrical and thermal conductivities in quenched and aged high-purity Cu-Ti alloys, Scripta Materialia, 48 (**2003**), 431–435, doi:10.1016/s1359-6462(02)00441-4

[10] W. A. Soffa, D. E. Laughlin, High-strength age hardening copper-titanium alloys: redivivus, Progress in Materials Science, 49 (**2004**), 347–366, doi:10.1016/s0079-6425(03)00029-x

[11] R. Markandeya, S. Nagarjuna, D. S. Sarma, Precipitation hardening of Cu-Ti-Cr alloys, Materials Science and Engineering A, 371 (**2004**), 291–305, doi:10.1016/j.msea.2003.12.002

[12] V. Lebreton, D. Pachoutinski, Y. Bienvenu, An investigation of microstructure and mechanical properties in Cu-Ti-Sn alloys rich in copper, Materials Science and Engineering A, 508 (**2009**), 83–92, doi:10.1016/j.msea.2009.01.050

[13] D. Božić, O. Dimčić, B. Dimčić, I. Cvijović, V. Rajković, The combination of precipitation and dispersion hardening in powder metallurgy produced Cu-Ti-Si alloy, Materials Characterization, 59 (**2008**), 1122–1126, doi:10.1016/j.matchar.2007.09.005

[14] S. Kim, M. Kang, Hydrogen production from methanol steam reforming over Cu-Ti-P oxide catalysts, Journal of Industrial and Engineering Chemistry, 18 (**2012**), 969–978. doi:10.1016/j.jiec.2011.10.009

[15] J. Liu, X. H. Wang, J. Chen, J. T. Liu, The effect of cold rolling on age hardening of Cu-3Ti-3Ni-0.5Si alloy, Journal of Alloys and Compounds, 797 (**2019**), 370-379, doi:10.1016/j.jallcom.2019.05.091

[16] G. Kresse, J. Furthmüller, Efficiency of ab-initio total energy calculations for metals and semiconductors using a plane-wave basis set, Computational Materials Science, 6 (**1996**), 15–50, doi:10.1016/0927-0256(96)00008-0

[17] P. Lang, T. Wojcik, E. Povoden-Karadeniz, C. D. Cirstea, E. Kozeschnik, Crystal structure and free energy of Ti_2Ni_3 precipitates in Ti-Ni alloys from first principles, Computational Materials Science, 93 (**2014**), 46–49, doi:10.1016/j.commatsci.2014.06.019

[18] X. M. Yuan, L. J. Zhang, Y. Du, W. Xiong, Y. Tang, A. J. Wang , S. H. Liu, A new approach to establish both stable and metastable phase equilibria for fcc ordered/disordered phase transition: application to the Al/Ni and Ni/Si systems, Materials Chemistry and Physics, 135 (**2012**), 94–105, doi:10.1016/j.matchemphys.2012.04.028

[19] D. Connétablea, O. Thomas, First-principles study of nickel-silicides ordered phases, Journal of Alloys and Compounds, 509 (**2011**), 2639–2644, doi:10.1016/j.jallcom.2010.10.118

[20] M. Tałach-Dumańska, P. Zięba, A. Pawłowski, J. Wojewoda, W. Gust, Practical aspects of discontinuous precipitation and dissolution, Materials Chemistry and Physics, 80 (**2003**), 476–481, doi:10.1016/s0254-0584(02)00550-3

[21] D. Kenta, G. Wang, W. Wang, M. S. Dargusch, Influence of ageing temperature and heating rate on the properties and microstructure of β Ti alloy, Ti-6Cr-5Mo-5V-4Al, Materials Science and Engineering A, 531 (**2012**), 98–106, doi:10.1016/j.msea.2011.10.040

[22] R. P. Carvalho, C. R. Miranda, A. F. Silva, The role of Cr on the electronic and optical properties of InCrN: A first principles study, Journal of Crystal Growth, 499 (**2018**), 13–17, doi:10.1016/j.jcrysgro.2018.07.021

[23] X. D. Zhan, W. Y. Huang, J. Y. Chen, C. Liu, H. Yu, L. J. Zhao, W. Jiang, Phase stability, elastic, anisotropic and thermodynamic properties of GdT_2Al_{20} (T=Ti, V, Cr) compounds: A first-principles study, Vacuum, 157 (**2018**), 312–319, doi:10.1016/j.vacuum.2018.09.001

[24] Q. Chen, Z. W. Huang, Z. D. Zhao, C. K. Hu, First-principles study on the structural, elastic, and thermodynamics properties of Ni_3X (X: Al, Mo, Ti, Pt, Si, Nb, V, and Zr) intermetallic compounds, Applied Physics A, 116 (**2014**), 1161–1172, doi:10.1007/s00339-013-8201-6

[25] C. Colinet, J. Tedenac, Enthalpies of formation of TM-X compounds (X=Al, Ga, Si, Ge, Sn). Comparison of ab-initio values and experimental data, Calphad, 54 (**2016**), 16–34, doi:10.106/j.calphad.2016.05.001

[26] M. Niranjan, Interface electronic structure and Schottky-barrier height in Si/NiSi(010) and Si/PtSi(010) heterostructures: A first principles theoretical study, Superlattices and Microstructures, 100 (**2016**), 808–817, doi:10.1016/j.spmi.2016.10.043